Proceedings of ASME Turbo Expo 2020
Turbomachinery Technical Conference and Exposition
GT2020
June 22-26, 2020, London, England

GT2020-15822

INVESTIGATION OF RECIRCULATING CASING TREATMENT FOR LOW-PRESSURE RATIO MIXED-FLOW MICRO-COMPRESSOR

Kewei Xu*
Gecheng Zha†
Department of Mechanical and Aerospace Engineering
University of Miami
Coral Gables, Florida 33124
Emails: kxx50@miami.edu , gzha@miami.edu

ABSTRACT

This paper investigates the recirculating casing treatment (RCT) of a low total pressure ratio micro-compressor to achieve stall margin enhancement while minimizing the design point efficiency penalty. Three RCT injection and extraction configurations are studied, including combined slot-duct, ducts only, and slot only. The numerical approach is validated with a tested micro-compressor using RCT. A very good agreement is achieved between the predicted speedlines and the measured results. To minimize the design point efficiency loss, it is observed that the optimal location of extraction and injection is where the recirculated flow rate can be minimized at the design point. To maximize stall margin, extraction location should favor minimizing the tip blockage such as at the location where the tip flow separation of the baseline blade is fully developed. In addition, the slot configuration that generates pre-swirl to the upstream flow is beneficial to improve stall margin due to reduced incidence. The highest stall margin enhancement achieved is 9.49% with the slot geometry that has the extraction at the 62%C chordwise location, but has a design point efficiency loss of 1.9%. Overall, a small efficiency penalty of 0.6% at the design point is achieved for the final design with the stall margin increased by 6.2%.

*Ph.D. Candidate
†Professor, ASME Fellow

NOMENCLATURE

AFC	Active Flow Control
C	Blade Tip Chord
CFJ	Co-flow Jet
MC	Micro-compressor
$\dot{m}$	mass Flow rate (kg/s)
m_{cor}	Corrected Mass Flow Rate, $\dot{m}\frac{\sqrt{T_0}}{p_0}$ (-)
TE	Trailing edge
LE	Leading edge
RCT	Recirculating casing treatment
n	RPM, round per minute
P_{tr}	Total pressure ratio
SM	Stall Margin
SMI	Stall Margin Improvement
ZNMF	Zero-net mass-flux
0	Total
1	Impeller Inlet
2	Impeller Outlet

INTRODUCTION

Co-flow Jet is a zero-net mass-flux (ZNMF) active flow control (AFC) method recently developed by Zha et al. [1–8] that has micro-compressors embedded inside the airfoil as actuators (Fig. 1). A CFJ airfoil withdraws flow from trailing edge, pressurizes it by the micro-compressor, and re-injects flow at leading

edge. It is demonstrated numerically and experimentally that CFJ achieves radical lift augmentation, drag reduction and stall angle of attack increase. The mixed type compressor is preferred to be used as the CFJ actuator due to its compact size and high flow capacity [8–12].

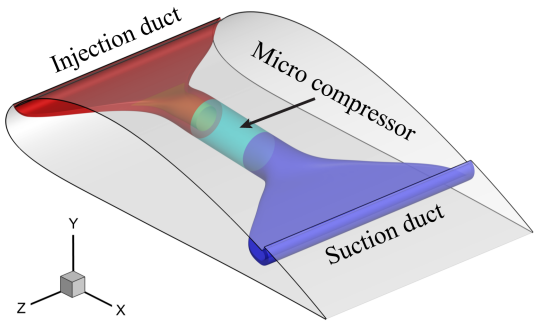

FIGURE 1: Schematics of the CFJ airfoil with embedded micro-compressor

In order to be operated in a wide flight envelope, the micro-compressor is required to have large operating range. Recirculating casing treatment (RCT) is demonstrated to be advantageous to extend the micro-compressor stall margin [12]. The RCT extracts separated flow from aft part of blade and injects near the leading edge. It can achieve significant stall margin improvement (SMI) with a small efficiency loss at the design point, and is therefore being studied widely.

D'andrea et al. [13] apply the pulsed air injection to control the rotating stall in a low speed axial flow compressor. It is observed experimentally that the technique is able to eliminate the hysteresis loop associated with rotating stall and improves the compressor operability range. Strazisar et al. [14] experimentally achieve 4% $\sim$ 6% stall margin improvement by re-injecting 0.7% $\sim$ 1.3% of main flow in a high loading transonic compressor stage. They study both steady and unsteady blowing and conclude that the unsteady injection can accomplish the same stall margin with the steady injection but with lower injection mass flow rate. A self-regulating casing treatment is proposed by Weichert et al. [15], which maximizes the recirculated flow rate at the stall point and minimizes the efficiency loss at the design point. The results show that 2.2% to 6.0% stall margin improvement are achieved for re-circulating 0.25% of the total compressor mass flow at near stall. The RCT mass flow rate is reduced by half at the design point. Similarly, a lossless casing treatment is designed by Djeghri et al. [16] for a mixed-flow compressor rotor to achieve noticeable stall margin improvement with no loss in peak efficiency. The design parameters with large effect include: open area ratio, slot skew angle, slot axial length and position. The slot recirculating casing treatment [17–21] is also widely studied on high pressure ratio centrifugal compressors, which utilizes pre-swirl for stall margin improvement.

In the previous studies [8–12], the RCT is implemented on the compressors with designed total pressure ratio of no less than 1.2, which creates a large pressure difference to drive the recirculation flow at near stall. Patel and Zha [12] observe that the micro-compressor they studied has little efficiency loss at the design point because there is almost no flow going through the RCT channels. The micro-compressor in the present paper is designed with a low total pressure ratio of 1.095 due to the CFJ flow control requirement. Such low pressure ratio makes the RCT design more challenging.

The purpose of this paper is to investigate the RCT geometric effects on a low pressure ratio mixed-flow micro-compressor to achieve significant stall margin improvement with a low efficiency loss at the design point. The studied geometrical parameters include the injection and extraction locations, RCT configurations of ducts, slot, and combined slot-duct.

NUMERICAL METHODS

As shown in Fig. 2, the computational domain has a single blade passage (blue), which consists of a converging intake, an impeller passage and a recirculating casing treatment. Fig. 2 (left) shows the structured mesh of the intake and impeller passage with a size of 0.47 million nodes. The impeller blade is meshed using O-grid topology in Turbogrid, which has 39 points in the blade span, 11 points at tip gap and 175 points around the blade. The wall spacing is set to make y^+ close to 1. Fig. 2 (right) shows the grid topology for the casing treatment. The slot geometry is meshed using structured H-grid with 0.1 million nodes for a single passage. For the duct geometry, the hybrid meshing, anisotropic tetrahedral extrusion (T-Rex) is used to generate a wall-refined unstructured mesh with 0.26 million cells. For the mesh refinement study, the meshes are refined by increasing the point number perpendicular to RCT wall and blade wall. The refined mesh size are 1.11, 0.91 and 1.21 million for the MC with three types of RCT (combined slot-duct, ducts, and slot), respectively. The mesh refinement study indicates that the solutions are converged based on the present mesh size.

The 3D Reynolds Averaged Navier-Stokes (RANS) equations are solved using ANSYS CFX code. The k-ω shear stress transport (SST) turbulent model is adopted. The advection terms are solved with 2nd order scheme. Total pressure, total temperature and flow direction are specified as inlet boundary conditions. Target exit mass flow rate is used as the outlet boundary condition to obtain the stable solutions near stall. Non-slip wall boundary condition is imposed on all solid walls. The frozen rotor boundary condition is applied on the interface between casing treatment and compressor casing. The interface between intake and impeller is treated with stage mixing boundary condition. The convergence criterion is that the residual reduced by 4 orders of

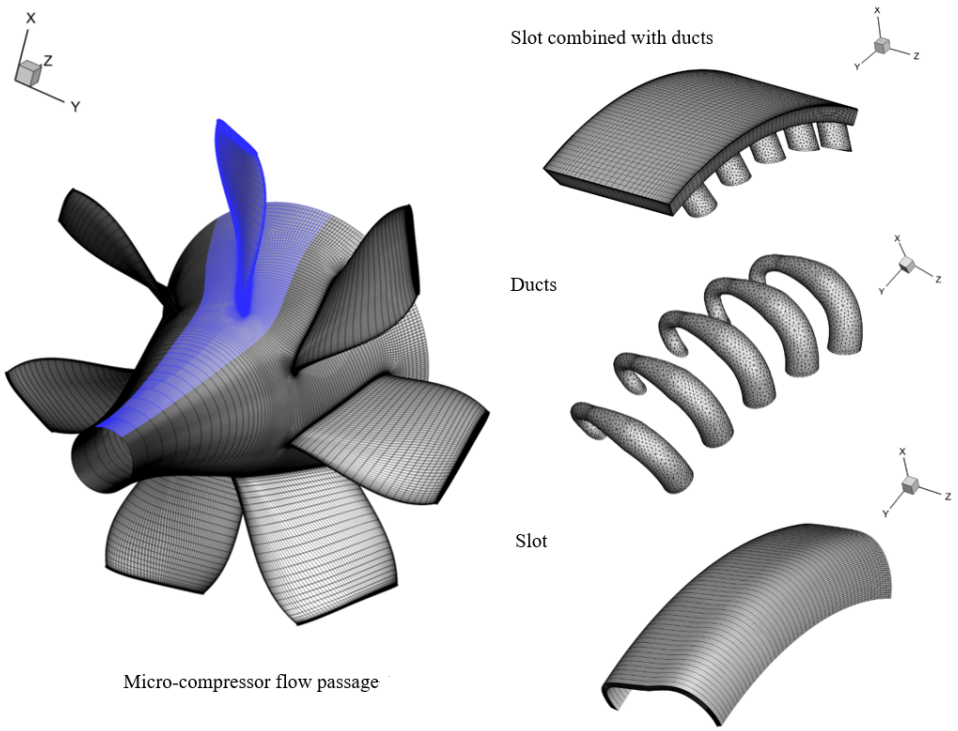

FIGURE 2: Computational meshes of the micro-compressor and casing treatment geometries

magnitude. In the near stall condition, such criterion is hard to reach due to the vortical flow in the casing treatment. Therefore, the computation is considered as converged when the mass flow becomes dynamically stable with time.

VALIDATION OF NUMERICAL METHODS

A rig tested micro-compressor with RCT [9, 10] is used to validate the numerical approach. The validated micro-compressor shown in Fig. 3 is a mixed-flow compressor using RCT to improve stall margin. Fig. 4 shows the streamlines in the RCT slot and ducts of the validated micro-compressor at near stall. Massive vortical flow is observed in the RCT chamber because of the cross-sectional area discontinuity between ducts and slot. The validated compressor has the similar size and Reynolds number with the micro-compressor studied in this paper. However, it has substantially lower mass flow rate and a higher total pressure ratio (P_{tr}). Its design point has total pressure ratio of 1.21 and isentropic efficiency of 80.2%. The computed speed-lines with the pressure ratio and efficiency are in good agreement with the measurements [10] as shown in Fig. 5, which has the mass flow rate normalized by the design point mass flow rate.

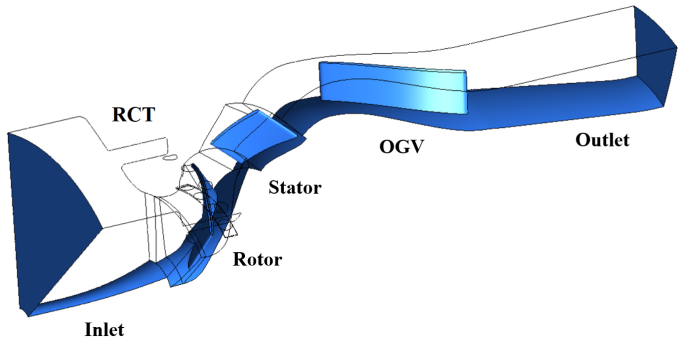

FIGURE 3: The configuration of the validated micro-compressor

The maximum discrepancy between the computed and measured pressure ratio and isentropic efficiency near stall are 2.32% and 2.1% respectively. The discrepancy is mostly due to the flow separation and complex vortical flow at near stall condition, for which the RANS turbulence model is inadequate to resolve.

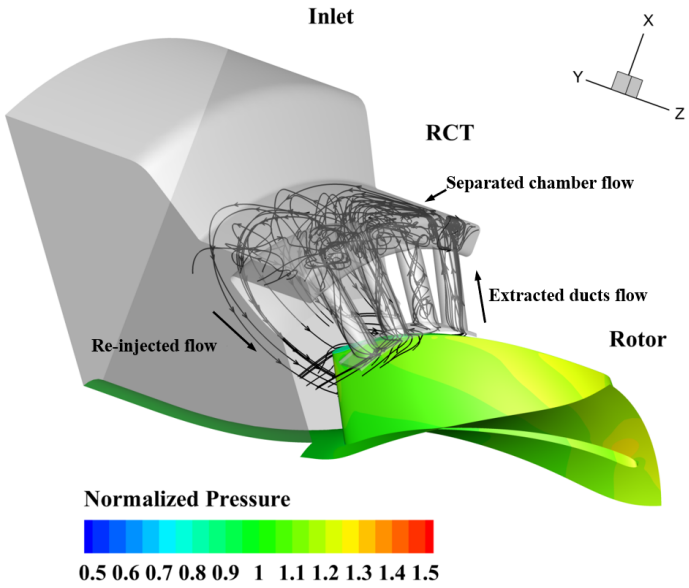

FIGURE 4: Streamlines and static pressure contour of the validated micro-compressor at near stall

THE BASELINE MICRO-COMPRESSOR

The baseline mixed-type single rotor micro-compressor with no casing treatment is designed following the methods described in [11]. The non-linear chordwise work distribution is adopted for the impeller blade to decrease the blade loading. Free vortex work distribution is applied for the rotor span to reduce spanwise mixing loss. The rotor designed efficiency achieves 87.1% with a low total pressure ratio of 1.095 and a high mass flow rate. The main geometrical parameters of the present micro-compressor is presented in the Table 1.

TABLE 1: Rotor Geometrical Parameters

Rotor inlet hub diameter	12.9mm
Rotor inlet casing diameter	42.4mm
Number of impeller blades	7

Fig. 6 and Fig. 7 present the computed speedlines at three normalized RPM ($n/\sqrt{T_{01}}$), 6279, 6849 and 7420. The designed speedline is at 6849, which provides the required mass flow rate and pressure ratio for co-flow jet airfoil flow control. The designed speedline of the baseline micro-compressor has 25.7% of stall margin defined by Eq. (1) and the RCT geometry studies are conducted for the designed RPM.

The stall margin is defined as:

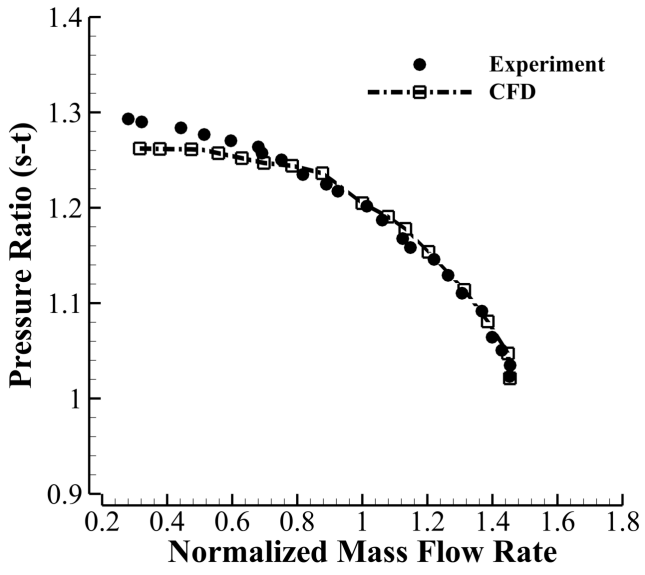

(a) Pressure ratio

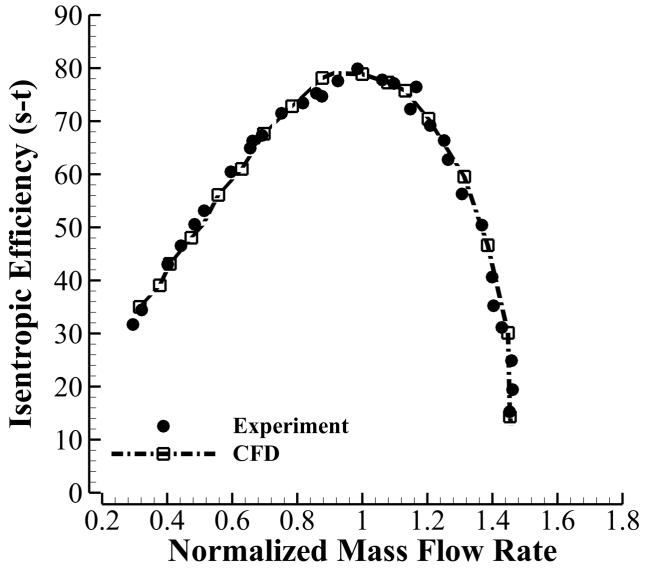

(b) Isentropic efficiency

FIGURE 5: Computed speedlines of a micro-compressor compared with the measured results [10]

$$SM = 1 - \left[\frac{(p_{02}/p_{01})_{design}}{(p_{02}/p_{01})_{stall}} \times \frac{m_{cor-stall}}{m_{cor-design}} \right] \quad (1)$$

where m_{cor} is the corrected mass flow rate defined by $\dot{m}\frac{\sqrt{T_0}}{p_0}$.

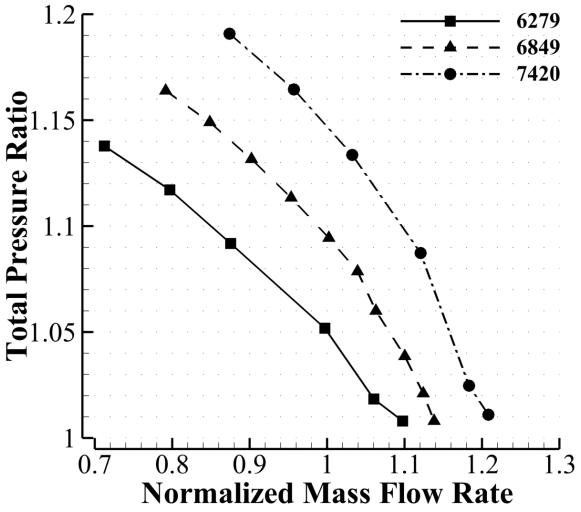

FIGURE 6: Computed speedlines of the baseline micro-compressor, pressure ratio [10]

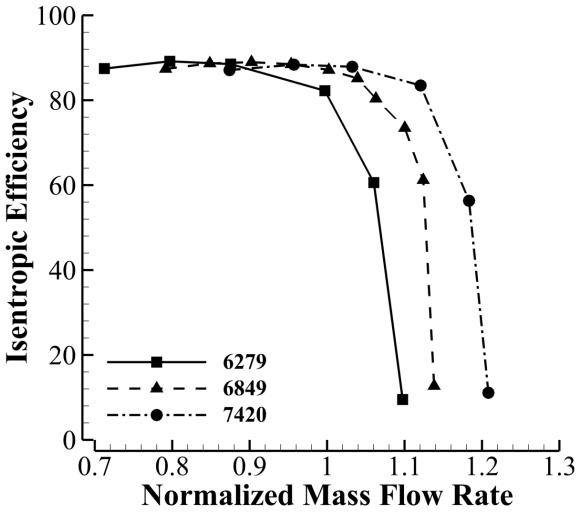

FIGURE 7: Computed speedlines of the baseline micro-compressor, isentropic efficiency [10]

ANALYSIS OF CASING WALL STATIC PRESSURE

The simple extraction/re-injection model [15] is adopted to locate the optimal RCT hole positions. The model calculates the pressure difference between RCT extraction and re-injection locations based on the shroud pressure distribution of the baseline compressor. It is desirable that the RCT hole locations make a minimal pressure difference between extraction and re-injection to preserve the design point efficiency. This is also consistent with the findings in [12]. Fig. 8 presents the tangentially-averaged static pressure on the baseline micro-compressor casing wall in the designed condition. As it shows, the static pressure is reduced rapidly as the inlet geometry converges. Partially attributed to the low loading of the impeller, it is difficult to find an upstream re-injection location near the blade leading edge that will generate a small pressure difference to minimize the design point efficiency loss. Therefore, the present study investigates various injection and extraction locations.

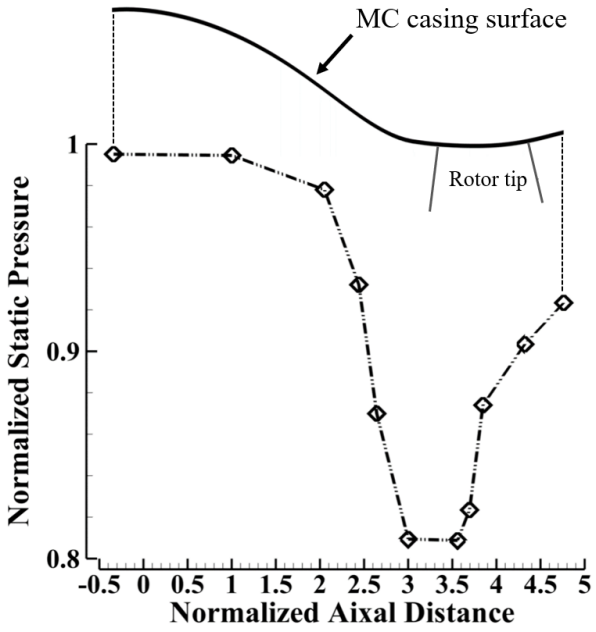

FIGURE 8: Static pressure distribution at the baseline micro-compressor casing

RECIRCULATING CASING TREATMENT RESULTS

Combined slot-duct configuration

Since the configuration of combined slot-duct RCT (see Fig. 2) is proved to be effective on the validated micro-compressor [9, 10, 12], such configuration is first studied. Fig. 9 shows the locations of extraction holes and injection slot for the three cases with different axial positions (red, blue and green), which all have the extraction angle of 60° about the axial direction. Extraction locations are labeled as "E" and injection locations are labeled as "I". Case 1 has the same injection location with Case 2 at 83%C upstream of the tip leading edge (LE), but has a more upstream extraction location at 62%C after tip blade LE. Case 2 has the same extraction location with Case 3 at 80%C downstream of the LE, but has the injection closer to tip LE.

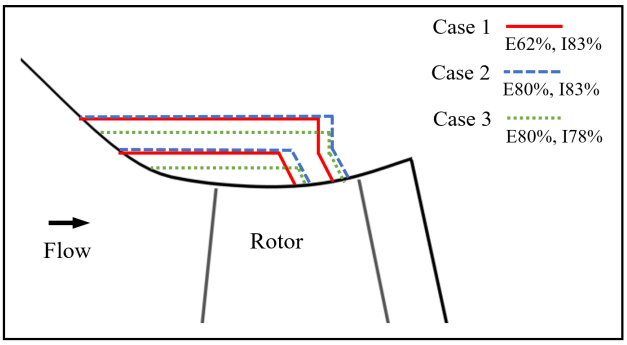

FIGURE 9: Schematics of the injection and extraction locations for the combined slot-duct RCT configuration

Fig.10 shows the speedlines of the micro-compressor with the three RCT geometries. It is shown that a noticeable stall margin improvement is achieved for all the three RCT designs. The highest stall margin improvement (SMI) of 6.4% is accomplished by Case 1, whereas Case 2 and 3 only improve the stall margin of 3.3% and 3.1% respectively. In terms of design point efficiency loss, Case 3 has the least penalty of 2.1% and Case 1 has the highest efficiency loss of 4.1%. This is because Case 3 extracts the flow near the blade trailing edge that has a high pressure, and injects at a low radius position that has a lower pressure than in Case 1 and 2. The pressure difference between injection and extraction for Case 3 is the lowest and hence also has the smallest recirculating flow at the design point.

Fig. 11 compares the Mach number contours and streamlines of the baseline, Case 1 and Case 2 micro-compressor at near stall condition. As it shows, a large flow separation occurs at the suction surface of the baseline micro-compressor, which creates a large blockage and induces stall. For the RCT cases, the tip blockage of Case 1 is significantly reduced as shown in Fig. 11 (b). Case 2 (Fig. 11 (c)) does not remove the blockage effectively and results in a lower stall margin compared with Case 1. It is also interesting to note that at near stall, Case 2 has a higher extraction pressure than Case 1 , which means Case 2 re-circulates higher amount of air flow. This suggests that case 2 should have a larger stall margin than case 1. However, the results in Fig.10 and Fig. 11 contradict to such statement.

The behavior of Case 1 and 2 is due to the difference of the extraction locations, which can be seen in Fig. 12 showing the tip region contours of the baseline MC with the RCT locations imposed. Fig. 12 (a) is the tip axial velocity contour, where the negative sign indicates the reversed flow and separation. It shows that the baseline micro-compressor has a tip separation core starting from 17%C to mid-chord. The extraction holes of Case 1 is located at 62%C, which is close to the severe flow separation. Extracting at such location is more effective than Case 2 at 80%C, which is far from the severe separation, even though it has

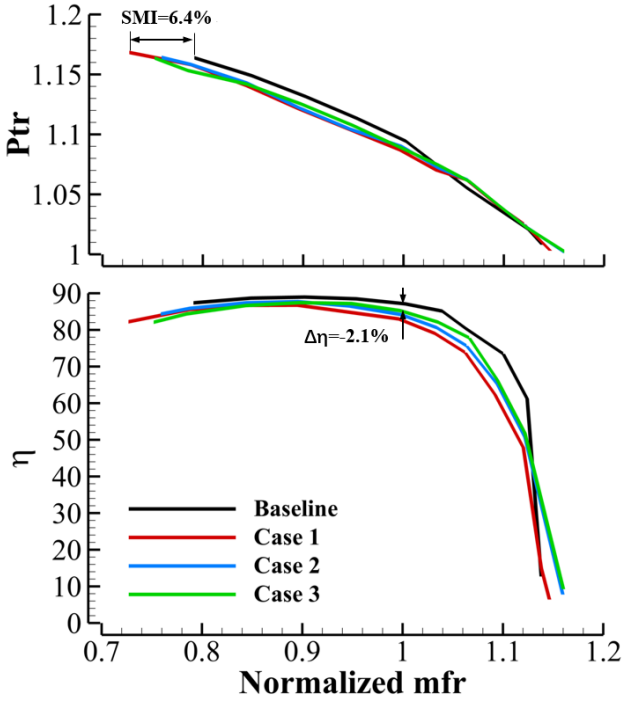

FIGURE 10: Speedlines of combined slot-duct RCT configuration

a higher extraction pressure as shown in Fig. 12 (b). This suggests that extraction location should be not only selected based on pressure difference, but also the relative location to tip separation.

The combined slot-duct RCT has a drawback that the flow channel area has a sudden expansion discontinuity, which creates a large loss for the recirculating flow. As shown in Fig. 13, the vortical flow occupies the slot chamber and reduces the flow capacity and the RCT effectiveness. Such flow structures also exists in the validated micro-compressor shown in Fig. 4. However, it works very well for that compressor with a high stall margin extension and a small design point efficiency penalty. It appears to be mostly due to its small pressure difference at the design point [12]. Therefore, the configuration of the next study removes the slot and only uses the ducts to connect the injection and extraction holes to avoid the area discontinuity.

Duct Configuration

Fig. 14 and Fig. 2 presents the geometries of the RCT with ducts only, labeled as Case 4 and Case 5. The two cases have the same injection and extraction locations, but the radius of the extraction hole in Case 4 is half of the radius in Case 5. The different extraction area creates a different flow capacity of circulating flow, which affects the effectiveness of RCT. Both Case 4 and 5 adopt the optimum extraction location of 62%C learned from

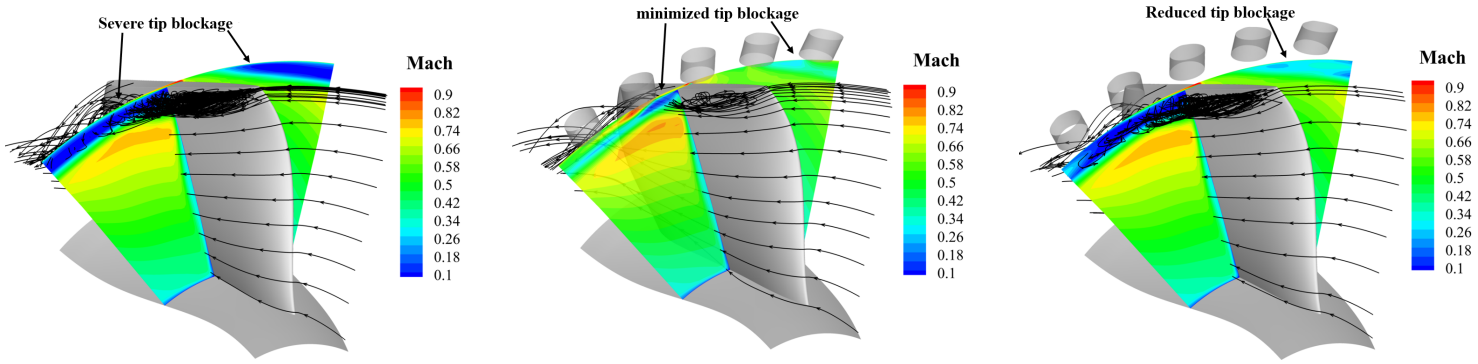

(a) Baseline (b) Case 1 (c) Case 2

FIGURE 11: Mach contours and streamlines of the micro-compressors

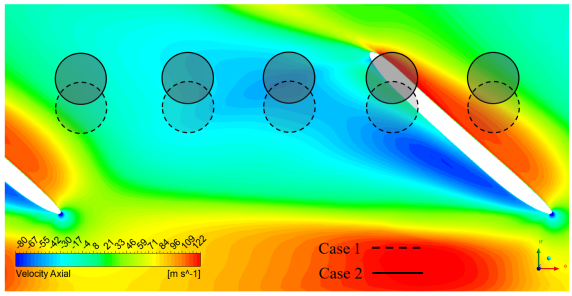

(a) Axial velocity contour

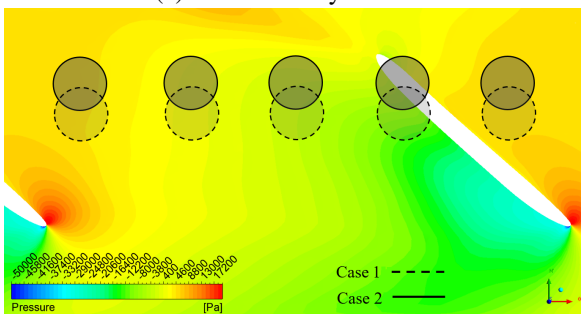

(b) Gage static pressure contour

FIGURE 12: Rotor tip contours of the baseline micro-compressor at near stall and RCT extraction location of Case 1 and Case 2

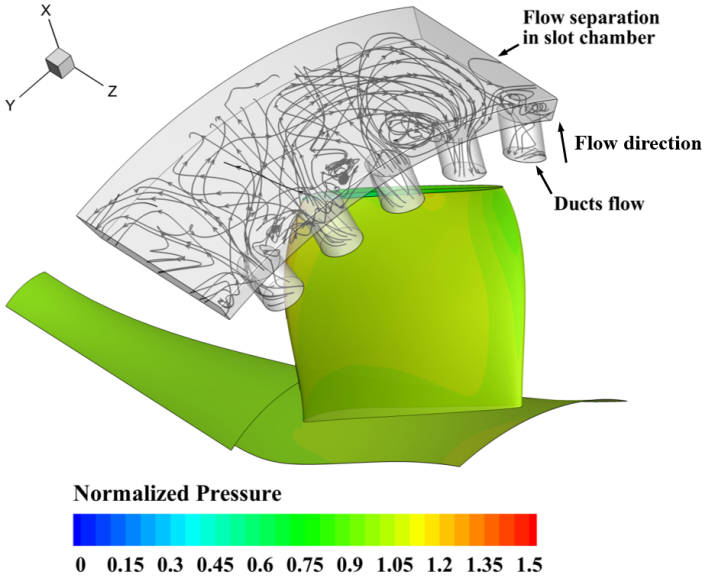

FIGURE 13: RCT streamlines of Case 1 at near stall condition

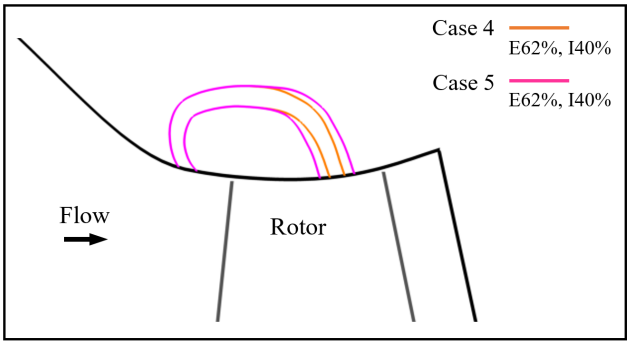

FIGURE 14: Schematics of the injection and extraction locations for the RCT with duct configuration

the previous combined slot-ducts studies. The injection holes are located at 40%C upstream of the tip blade leading edge. The extraction and injection holes are angled 60 deg about the axial direction.

The speedlines of the ducts only RCT configurations are presented in Fig. 15. Both cases can accomplish a significant stall margin improvement about 6.2%. A very minor efficiency penalty of 0.6% is obtained for Case 4 due to the smaller amount of recirculated mass flow rate of 0.24% of the compressor mass flow. Case 5 has a larger efficiency loss of 0.84% due to the

higher re-circulated mass flow rate caused by the larger extraction area. Compared with the combined slot-duct RCT configuration, the ducts only configuration has a similar stall margin improvement, but substantially less penalty of design point efficiency loss.

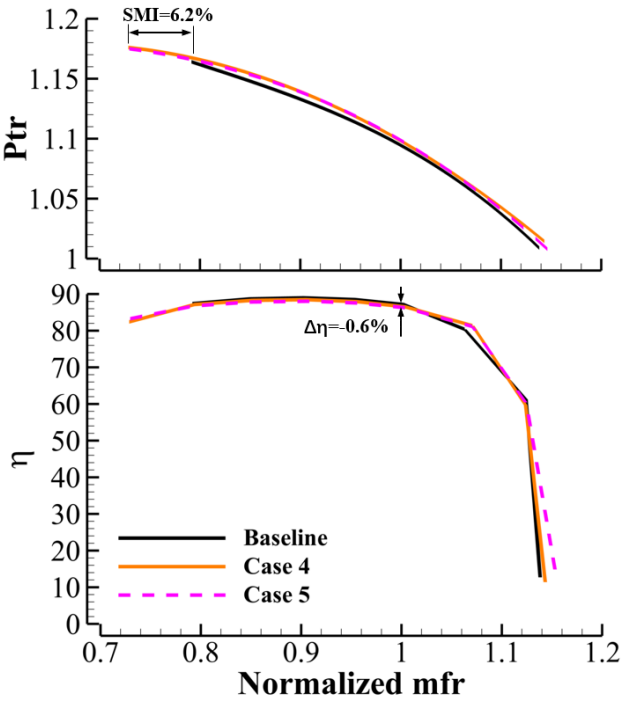

FIGURE 15: Speedlines of RCT duct configuration

The swirl angle used in this paper is the arctangent of the relative circumferential velocity divided by the meridional velocity of the flow. Fig.16 presents the spanwise swirl angle distribution upstream of the impeller blade for the baseline, Case 4 and Case 5 at the near stall condition. The swirl angle is slightly decreased about 2° near the tip. In general, it is desirable that the RCT injects a swirled flow to the upstream and generates some pre-swirl to decrease the tip incidence and improve the compressor stall margin. However, in ducts only RCT, the circumferential momentum of the extracted flow is reduced by the duct wall and little swirl effect is passed to the upstream. To further increase the stall margin, the slot RCT configuration is implemented in the next study.

Slot Configuration

The RCT slot configuration (Case 6) is studied in this section. As shown in Fig. 17 and Fig. 2, the extraction and injection are connected by a circumferential slot. The optimum location of

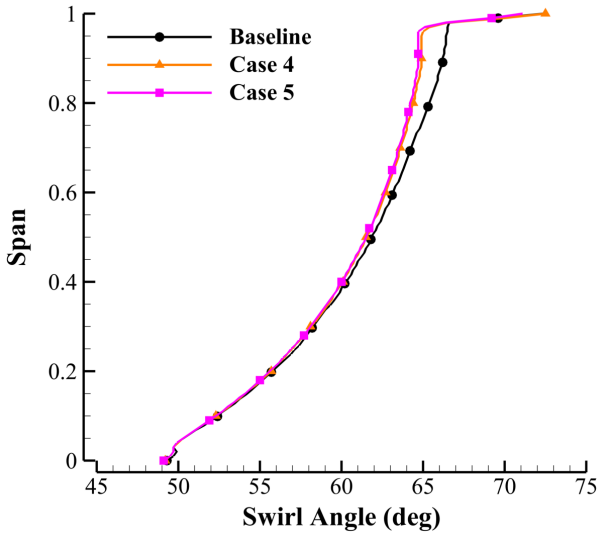

FIGURE 16: Swirl angle distributions upstream of the impeller blade at near stall

62%C is adopted for the extraction slot to better remove tip separation. The injection slot is located at 40%C upstream of the tip LE. The injection and extraction angles are 60° about the axial direction, the same as the duct only cases.

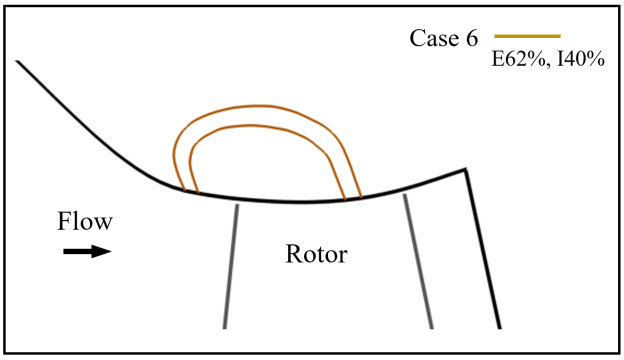

FIGURE 17: Schematics of the injection and extraction locations for the RCT with slot configuration

Fig. 18 presents the speedlines of the Case 6 micro-compressor. A stall margin improvement of 9.49% is achieved, which is the highest among the six cases. It is not only because of the optimum extraction location but also because of the pre-swirl generated by the slot geometry. As shown in Fig.19, the spanwise swirl angle distribution indicates that the swirl angle is reduced about 10° near the tip region for Case 6. The slot geometry is able to preserve and transfer the circumferential mo-

mentum to the upstream. During the mixing with the upstream flow, the circulated flow decreases the circumferential velocity of the main flow and mitigates the swirl angle. Fig. 20 shows a clear reduction of circumferential velocity in Case 6 compared with the baseline micro-compressor. Fig. 18 also indicates that the design point efficiency of Case 6 suffers a penalty of 1.9%, which is due to re-circulating flow at the design point.

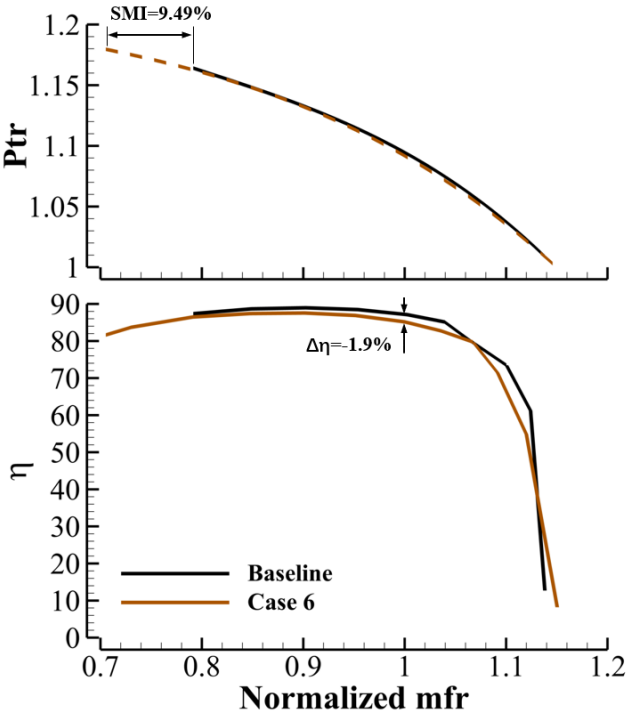

FIGURE 18: Speedlines of RCT slot configuration

The performance of the six RCT cases are presented in table 2, including stall margin improvement, efficiency penalty and re-circulated mass flow rate at design condition. The minimum efficiency penalty is achieved in Case 4 with duct configuration. The slot configuration, Case 6 has the highest SMI of 9.49% due to the pre-swirl effects. Note that the negative sign of RCT flow rate means the flow is not extracted from the extraction duct (holes, slot) but enters it due to the high pressure at the injection duct (holes, slot) location at the design point. This reversed RCT flow mixes with tip flow and significantly reduces rotor efficiency in Case 1 to 3.

In terms of the desirable design for CFJ, the one with the least efficiency penalty is preferred, that is Case 4. One of the major goals for CFJ is to achieve low energy consumption. Therefore, preserving efficiency is more important than improving stall margin for the CFJ micro-compressor. The other reason is that CFJ does not necessarily require a very large stall margin. As shown in Fig. 21, the CFJ injection duct connects the micro-compressor with airfoil leading edge (LE), which transfers the low static pressure at airfoil suction surface to the micro-compressor outlet and serves as the compressor back pressure. Therefore, the micro-compressor tends to be pushed to operate at a high mass flow condition, which is away from the near stall condition.

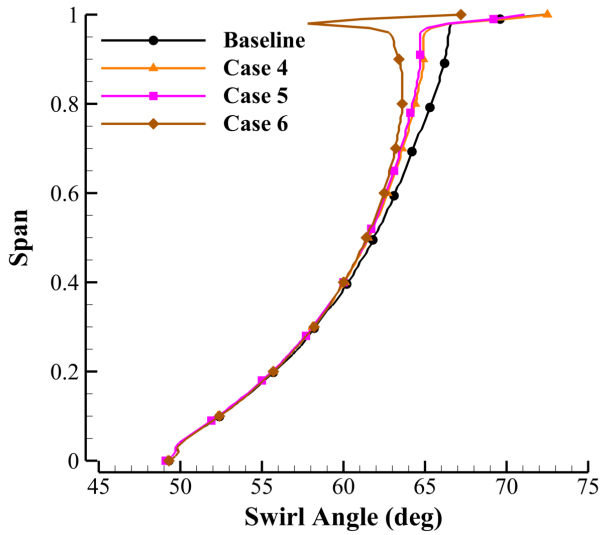

FIGURE 19: Swirl angle distributions upstream of the impeller blade at near stall

TABLE 2: Summary of RCT performance

Cases	SMI	$\Delta\eta$	RCT flow rate (design point)
1	6.4%	-4.1%	-2.2%
2	3.3%	-2.3%	-2.3%
3	3.1%	-2.1%	-1.2%
4	6.2%	-0.6%	0.24%
5	6.2%	-0.84%	0.4%
6	9.49%	-1.9%	0.5%

CONCLUSIONS

This paper investigates the recirculating casing treatment (RCT) of a low total pressure ratio micro-compressor to achieve stall margin enhancement while minimizing the design point efficiency penalty. Various RCT injection and extraction configurations are studied, including combined slot-duct, ducts only,

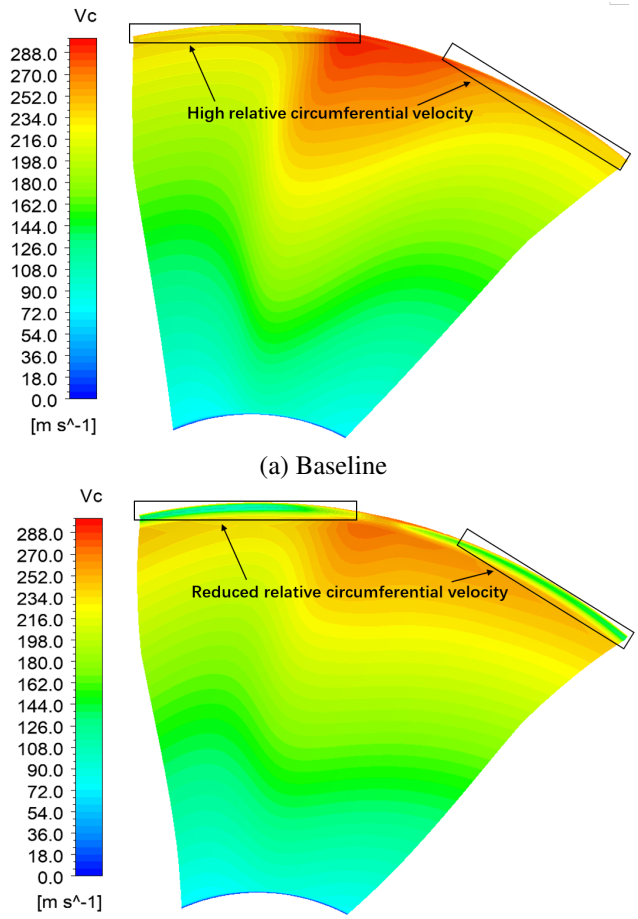

(a) Baseline

(b) Case 6

FIGURE 20: Relative circumferential velocity contours upstream of the rotor blade

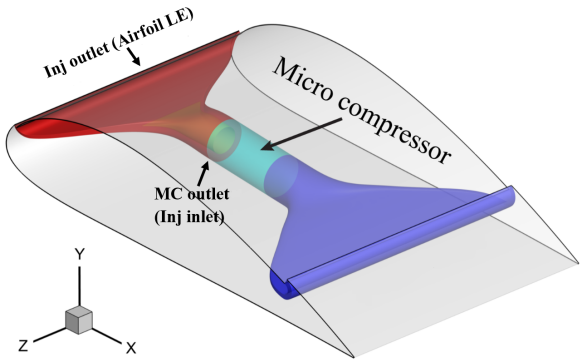

FIGURE 21: Illustration of the positions of injection duct and micro-compressor

and slot only. To minimize the design point efficiency loss, it is observed that the optimal location of extraction and injection is where the recirculated flow rate can be minimized at the design point. To maximize stall margin, extraction location should favor minimizing the tip blockage such as at the location where the tip separation is fully developed. In addition, the slot configuration that generates pre-swirl to the upstream flow is beneficial to improve stall margin. Overall, a small efficiency penalty of 0.6% at the design point is achieved for the duct only geometry with the stall margin increased by 6.2%. The highest stall margin enhancement achieved is 9.49% with the slot geometry but has a large design point efficiency penalty of 1.9%.

ACKNOWLEDGMENT

We thank the fruitful discussion with Dr. Chris Robinson at PCA Engineers regarding the numerical approaches to simulate the micro-compressor with re-circulating casing treatment.

REFERENCES

[1] Zha, G.-C., F Carroll, B., Paxton, C. D., Conley, C. A., and Wells, A., 2007. "High-performance airfoil using coflow jet flow control". *AIAA journal,* ***45***(8), pp. 2087–2090.

[2] Lefebvre, A., Dano, B., Bartow, W., Fronzo, M., and Zha, G., 2016. "Performance and energy expenditure of coflow jet airfoil with variation of mach number". *Journal of Aircraft,* ***53***(6), pp. 1757–1767.

[3] G. Zha, W. Gao, and C.D. Paxton, 2007. "Jet Effects on Co-Flow Jet Airfoil Performance". *AIAA Journal,* ***45***, pp. 1222–1231.

[4] G.-C. Zha, C. Paxton, A. Conley, A. Wells, nd B. Carroll, 2006. "Effect of Injection Slot Size on High Performance Co-Flow Jet Airfoil". *AIAA Journal of Aircraft,* ***43***, pp. 987–995.

[5] Yang, Yunchao and Zha, Gecheng, 9-13 January 2017. "Super-Lift Coefficient of Active Flow Control Airfoil: What is the Limit?". *AIAA Paper 2017-1693, AIAA SCITECH2017, 55th AIAA Aerospace Science Meeting, Grapevine, Texas*, p. 1693.

[6] Jinhuan, Z., Kewei, X., Yang, Y., Ren Yan, P. P., and Zha, G., 2018. "Aircraft control surfaces using co-flow jet active flow control airfoil". *AIAA Aviation and Aeronautics Forum and Exposition 2018*.

[7] Kewei, X., Jinhuan, Z., and Zha, G., 2019. "Drag minimization of co-flow jet control surfaces at cruise conditions". *AIAA Science and Technology Forum 2019*.

[8] Zha, G., Yang, Y., Ren, Y., and McBreen, B., 2018. "Super-lift and thrusting airfoil of coflow jet actuated by micro-compressors". In 2018 Flow Control Conference, June 25-29, 2018, Atlanta, Georgia, pp. AIAA Paper–2018–3061.

[9] Robison, C., Feb. 23, 2017. "Design of a mixed flow fan". Vol. PCA-211-3-rep1-1, PCA Engineering Limited.
[10] Zwyssig, C., Oct. 24, 2017.. "Design of a mixed flow fan prototype". Vol. PR-4241-011, Celereton.
[11] Xu, K., and Zha, G., 2019. "Design of high specific speed mixed flow micro-compressor for co-flow jet actuators". In ASME Turbo Expo 2019: Turbomachinery Technical Conference and Exposition, American Society of Mechanical Engineers Digital Collection,GT2019-90980.
[12] Patel, P., and Zha, G., 2019. "Investigation of mixed micro-compressor casing treatment using non-matching mesh interface". In ASME Turbo Expo 2019 Turbomachinery Technical Conference and Exposition, GT2019-90977, American Society of Mechanical Engineers.
[13] Dandrea, R., Behnken, R., and Murray, R., 1997. "Rotating stall control of an axial flow compressor using pulsed air injection". *Journal of turbomachinery,* ***119***, pp. 742–752.
[14] Strazisar, A. J., Bright, M. M., Thorp, S., Culley, D. E., and Suder, K. L., 2004. "Compressor stall control through endwall recirculation". In ASME Turbo Expo 2004: Power for Land, Sea, and Air, GT2004-54295, American Society of Mechanical Engineers, pp. 655–667.
[15] Weichert, S., Day, I., and Freeman, C., 2011. "Self-regulating casing treatment for axial compressor stability enhancement". In ASME 2011 turbo expo: turbine technical conference and exposition, GT2011-46042, American Society of Mechanical Engineers Digital Collection, pp. 225–237.
[16] Djeghri, N., Vo, H. D., and Yu, H., 2015. "Parametric study for lossless casing treatment on a mixed-flow compressor rotor". In ASME Turbo Expo 2015: Turbine Technical Conference and Exposition, GT2015-42750, American Society of Mechanical Engineers Digital Collection.
[17] Tamaki, H., 2012. "Effect of recirculation device with counter swirl vane on performance of high pressure ratio centrifugal compressor". *Journal of Turbomachinery,* ***134***(5).
[18] Sivagnanasundaram, S., Spence, S., Early, J., and Nikpour, B., 2013. "An impact of various shroud bleed slot configurations and cavity vanes on compressor map width and the inducer flow field". *Journal of Turbomachinery,* ***135***(4), p. 041003.
[19] Chen, H., and Lei, V.-M., 2013. "Casing treatment and inlet swirl of centrifugal compressors". *Journal of Turbomachinery,* ***135***(4), p. 041010.
[20] Jung, S., and Pelton, R., 2016. "Numerically derived design guidelines of self recirculation casing treatment for industrial centrifugal compressors". In ASME Turbo Expo 2016: Turbomachinery Technical Conference and Exposition, GT2016-56672, American Society of Mechanical Engineers Digital Collection.
[21] Favaretto, C. F. F., Anderson, M. R., Li, S., and Hu, L., 2018. "Development of a meanline model for preliminary design of recirculating casing treatment in turbocharger compressors". In ASME Turbo Expo 2018: Turbomachinery Technical Conference and Exposition, GT2018-75717, American Society of Mechanical Engineers Digital Collection.